Understanding the plasmonics of nanostructured atomic force microscopy tips

A. Sanders, R. W. Bowman, L. Zhang, V. Turek, D. O. Sigle, A. Lombardi, L. Weller, and J. J. Baumberg[a)]
Nanophotonics Centre, Department of Physics, Cavendish Laboratory, Cambridge CB3 0HE, United Kingdom

(Received 14 September 2016; accepted 25 September 2016; published online 12 October 2016)

Structured metallic tips are increasingly important for optical spectroscopies such as tip-enhanced Raman spectroscopy, with plasmonic resonances frequently cited as a mechanism for electric field enhancement. We probe the local optical response of sharp and spherical-tipped atomic force microscopy (AFM) tips using a scanning hyperspectral imaging technique to identify the plasmonic behaviour. Localised surface plasmon resonances which radiatively couple with far-field light are found only for spherical AFM tips, with little response for sharp AFM tips, in agreement with numerical simulations of the near-field response. The precise tip geometry is thus crucial for plasmon-enhanced spectroscopies, and the typical sharp cones are not preferred. *Published by AIP Publishing.*
[http://dx.doi.org/10.1063/1.4964601]

Within the last decade, nano-optics has benefited from the advent of metallic tip-based near-field enhancement techniques such as tip-enhanced Raman spectroscopy (TERS) and scanning near-field microscopy (SNOM), leading to demonstrations of single molecule detection[1] and spatial mapping of chemical species.[2] Despite their high spatial resolution and scanning capabilities, there remains confusion about the plasmonic response of metallic tips. Tip systems built on atomic force microscopy (AFM) probes can exhibit electric field enhancements close to 100 at the apex (Raman enhancements up to 10^8),[2] due to a combination of plasmonic localisation and a non-resonant lightning rod effect. The factors determining a tip's ability to enhance the near-field include the experimental excitation/collection geometry, tip sharpness, surface metal morphology, and constituent material.

Despite large measured near-field enhancements, the standard sharp AFM tip geometry does not support radiative plasmons. The extended ($\sim$20 μm) size and single curved metal-dielectric interface of an AFM tip supports only weakly confined localised surface plasmons (LSPs)[3] and propagating surface plasmon polaritons (SPPs), which may be localised by adiabatic nanofocussing.[4–9] Lack of a dipole moment means that neither LSPs or SPPs strongly couple with radiative light in the same manner as multipolar plasmons in sub-wavelength nanoparticles (NPs).[3] For this reason, the tip near-field is often excited with evanescent waves[10] or via nanofabricated gratings[6] to access the optically dark SPPs, with resonant scattering of evanescent waves,[11–13] resonances in the TERS background[14,15] and depolarised scattering images[16] providing evidence for localised plasmon excitation. For Au tips, such plasmon resonances are typically found between 600 and 800 nm.

Improvements in enhancement are often found in roughened tips with grains acting as individual nano-antennae for more confined LSPs, however, this approach lacks reproducibility.[16] In recent years, controlled nanostructuring of the tip apex with a distinct sub-wavelength-size metallic feature has been explored in order to engineer and tune a plasmonic optical antenna precisely at the apex and better incorporate more localised multipolar plasmons.[16–21] Etching,[21,22] focussed-ion-beam machining,[23–25] selective deposition,[26] nanoparticle pickup,[27] nanostructure grafting[28] and electrochemical deposition[29] have all been used to nanostructure the optical antenna tips.

Scattering resonances in the visible-NIR spectrum have been directly measured on a subset of these[25,26,29] while other reports use improvements in the field enhancement as a measurement of antenna quality.[20,21,28] In such cases, the field enhancement has been attributed to give improvements by an order of magnitude through plasmon excitation.[20,23,24,29]

The simplest geometry for a tip apex is a spherical nanoparticle (NP), giving LSPs similar to those in an isolated spherical metallic nanoparticle. In this paper we demonstrate an effective method for characterising the radiative plasmon modes of a tip and clearly show the benefits of utilising spherically nanostructured tips as near-field enhancers.

The optical properties of AFM tips are studied using a custom-built confocal microscope with a supercontinuum laser source for dark-field scattering spectroscopy (Fig. 1). Both illumination and collection share the optical axis of a 0.8 NA IR objective. Supercontinuum laser light is filtered into a ring and incident on a tip at 0.6–0.8 NA while light scattered by the tip is confocally collected from the central laser focus using an iris to restrict the collection NA below 0.6. Broadband polarising beamsplitters are used to simultaneously measure spectra which are linearly polarised both along the tip axis (axial) and perpendicular to the tip axis (transverse).

A scanning hyperspectral imaging technique is applied to determine the local optical response at the tip apex. Tips are raster scanned under the laser spot and the dark field scattering from the confocal sampling volume measured at each point, forming a hyperspectral data cube. Images are formed at each wavelength contained in the cube, with each image pixel digitised into 1044 wavelengths between 400 and

a)Email: jjb12@cam.ac.uk. URL: www.np.phy.cam.ac.uk

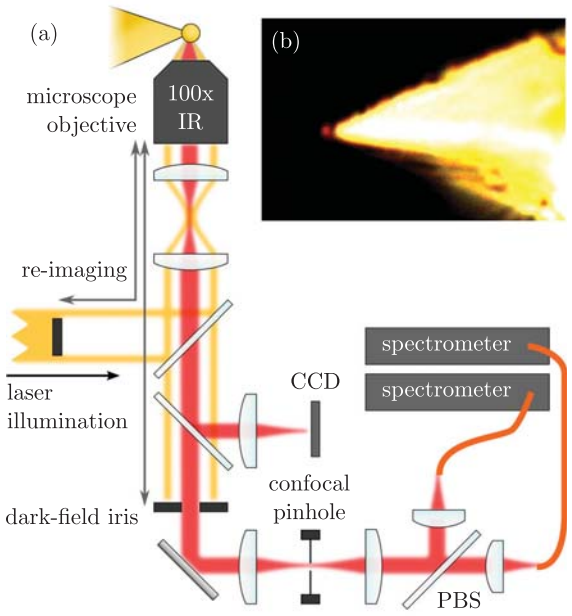

FIG. 1. (a) Hyperspectral imaging with supercontinuum laser focussed onto the tip apex for imaging, and the tip is raster scanned across the beam with scattering spectra of both polarisations acquired at each position. (b) Spherical tip imaged in dark-field microscopy.

1200 nm. Measured spectra are normalised to a spectrum of flat metal of the same material to show only structural effects. Image slices at individual wavelengths or wavelength bands are then readily constructed to display localised spectral features. Fast image acquisition is made possible by the high brightness supercontinuum laser source (100 μW μm^{-2}) and cooled benchtop spectrometers, enabling 10 ms integration times (5 min per image). Within plasmonics, this approach to hyperspectral imaging has been used to identify distributed plasmon modes in aggregated AuNP colloids[30] and to image SPPs.[31] Radiative plasmons can be spatially identified with a resolution of around 250 nm using this technique.

To investigate the radiative plasmonic properties of nanostructured tips, hyperspectral images are taken of both standard (sharp) and spherical-tipped Au AFM tips. Spherical tips are either 300 nm in diameter, 50 nm Au-coated NanoTools B150 AFM probes or electrochemically deposited AuNP-on-Pt AFM probes, fabricated in-house[29] (shown in Fig. 2). Fabricated tips are pre-treated where possible prior to use with ambient air plasma and/or piranha solution to remove organic surface residue and, in some cases, smooth out surface roughness.

Comparisons between spherical- and sharp-tipped Au probes using hyperspectral image slices (Fig. 3) show that spherical tips exhibit a characteristic red (600–700 nm) scatter, separated from the bulk tip. No similar localised scattering is seen in the visible spectrum with sharp Au tips, which have a ten-fold weaker optical response and appear similar to non-plasmonic Pt tips. This delocalised apex scatter can also be directly seen in dark-field microscopy images (Fig. 1(b)). The AuNP-on-Pt structure behaves very similarly to the Au-coated spherical tip (which has a diamond-like-carbon inside), likely because the 50 nm coating thickness is greater than the skin depth.[32,33] As we show below, differences in plasmon resonances arise due to the Au-Pt and Au-Au neck boundaries.

Integrating spectra around each tip better shows the 600–700 nm scattering resonance from spherical Au tips (Figs. 3(d) and 3(e)), which are reliably present in all spherical-tipped AFM probes, both vacuum-processed and electrochemically deposited. We attribute these to localised surface plasmon excitation, while electron microscopy confirms this resonance correlates only with spherical Au tip shapes. The response of sharp Au tips shows no similar plasmonic features, while the slow rise in scattering towards the near-infrared (NIR) is consistent with lightning rod scattering.[3]

Broadband tuneable surface-enhanced Raman scattering (SERS) measurements[34] confirm that the optical scattering resonance seen in spherical Au tips is indeed caused by radiative plasmon excitation. The trapped plasmon fields enhance optical processes on the surface such as surface-enhanced Raman scattering (SERS) and here we use the SERS background[34,35] as a reporter of the plasmonic near-field strength. SERS background spectra are integrated across a range of excitation wavelengths between 500 and 700 nm, spaced 10 nm apart, to extract any scattering resonances. The resulting spectrum (Fig. 3(f)) shows a distinct peak around the spherical Au tip scattering resonance, while no such resonance is seen for sharp Au tips. Further confirmation stems from direct observation of plasmon coupling between spherical tips, as has been previously reported.[36]

Plasmon resonances in spherical AuNP tips correspond to *radiative* antenna-like modes, similar to those in plasmonic nanoparticles, that efficiently couple far-field light into strong collective free electron oscillations without the need for SPP momentum matching. As with nanoparticles, the signature of these plasmons is an optical resonance indicating their large dipole moment (Fig. 3(d)). Such radiative plasmons only form if multipolar surface charge oscillations are supported, requiring a structure with multiple metal-dielectric interfaces.

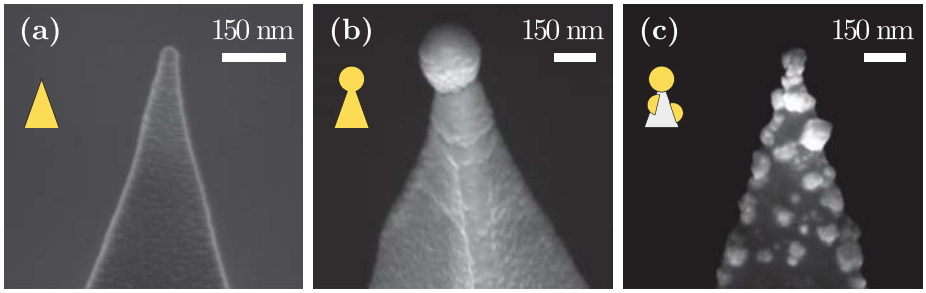

FIG. 2. SEM images of (a) sharp Au AFM tip, (b) Au-coated spherical AFM tip (Nanotools), and (c) electrochemically deposited AuNP-on-Pt AFM tip.

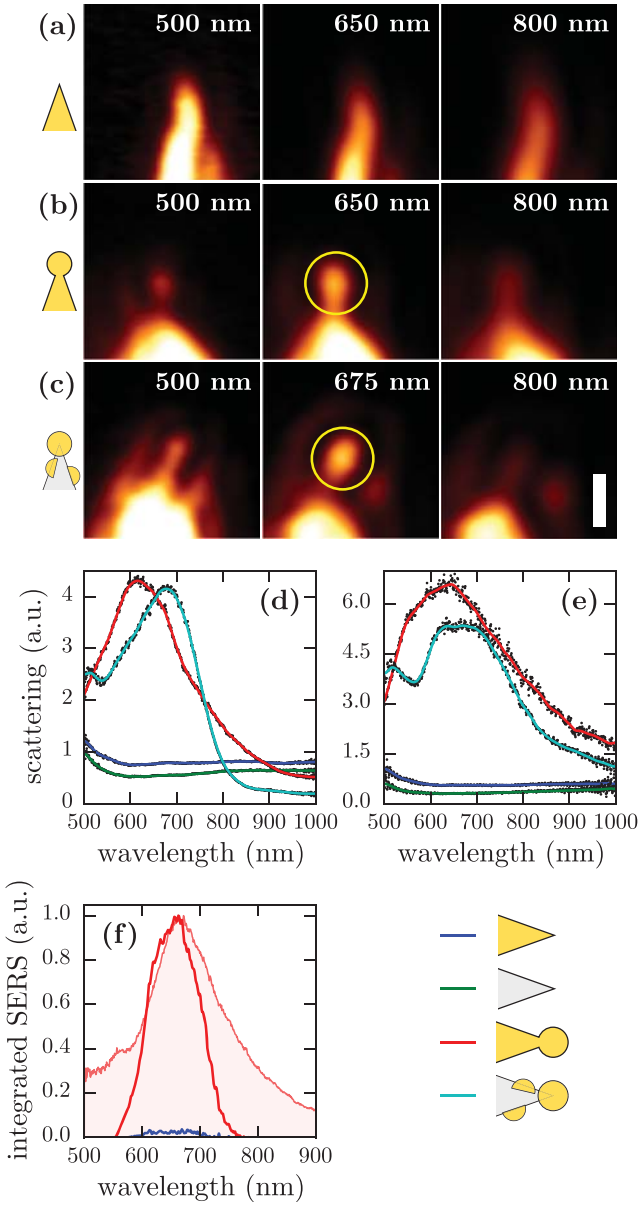

FIG. 3. Hyperspectral images of (a) sharp Au tip, (b) Au-coated spherical tip (Nanotools), and (c) electrochemically deposited AuNP-on-Pt tip. Collected light is polarised along tip axis, colour maps all have the same normalisation. Scale bar is 600 nm. (d), (e) Scattering spectra of both sharp and spherical metal tips, extracted from hyperspectral images around the apex region, in (d) axial and (e) transverse polarisations. (f) Integrated SERS background from sharp and spherical Au tips. Scattering spectrum of spherical Au tip apex shown shaded.

Since spherical metallic tips possess a neck behind the tip, they can support NP plasmonics. Sharp tips do not have this back surface, hence cannot support radiative plasmon resonances, although the single metal-dielectric surface supports launching of evanescent SPPs and a strong lightning rod component.

Simulated near-field spectra (using the boundary element method) around the apex of 300 nm spherical Au and AuNP-on-Pt tips with 120 nm neck diameters ($d_{neck} = 0.4d_{sphere}$) are shown in Fig. 4(a). Tips are simulated with a length of 1.88 μm to avoid truncation artefacts which are commonly seen in tip simulations and erroneously suggest plasmonic performance even in sharp tips. Strong modes appear along the tip axis for all spherical tips between 550 and 700 nm, as in experiments with peak wavelengths that match our hyperspectral results. Near-field maps corresponding to the main resonance in each tip (Figs. 4(b) and 4(c)) show dipole-like resonances with the neck spatially splitting the underside of each mode, mixing it with quadrupolar modes and shifting it towards the blue.

In order to directly compare the *plasmonic* behaviour of spherical and sharp Au tips independent of lightning rod contributions, the neck width is incrementally increased. This allows us to study structures which smoothly transition from a nanoparticle attached to the apex of a sharp Au tip, into a rounded tip geometry, without the apex radius ever changing. The field enhancement and peak positions extracted from this morphology transition (Fig. 4(d)) show resonances insensitive to the neck width until $d_{neck} > 0.8d_{sphere}$, explaining the robustness of observed spherical tip plasmons between different tip morphologies. However, a steady decrease in the field enhancement is observed once $d_{neck} > 0.4d_{sphere}$, decreasing faster once $d_{neck} > 0.8d_{sphere}$. This supports the claim that sharp tips cannot sustain antenna-like plasmons and that the majority of enhancement is from lightning rod effects. We note that the lateral spatial localisation of the field approaches $0.3d_{sphere}$ independent of this neck diameter.

These results demonstrate the importance of considering which plasmons might exist in a particular experiment and nanostructure geometry, and that it is vital to characterise nanostructures prior to their application. Apex nanostructuring can controllably introduce radiative plasmons into the tip geometry, lifting the evanescent illumination restriction of sharp tips and permitting use of a wider range of microscope configurations. While the lightning rod effect will always contribute to the field enhancement and favour sharp tips, exploiting resonant plasmonic enhancement in a carefully optimised spherical tip can further improve the near-field enhancement. The spherical tip geometry and materials shown here are optimised for use with the typically used 633 nm laser wavelengths.

Demonstrated interactions between spherical tip plasmons[36] also suggest coupling with an image charge in a planar surface is possible and could be used in nanometric tip-surface gaps to further localise the field on resonance with near infrared lasers. Exploiting radiative tip plasmons in this manner bridges the gap between SERS and conventional TERS, forming a spatially mappable version of the nanoparticle-on-mirror geometry.[37,38] These systems repeatedly produce Raman enhancements of up to 10^7 with nanometric mode volumes, much like tips, and demonstrate that plasmonic gaps can exhibit comparatively large field enhancements without relying only on the lightning rod effect.

Secondly, without prior knowledge of the tip-system spectral response, it is difficult to properly interpret any measurements, such as TERS spectra. Improved tip characterisation is crucial to understanding variations in TERS spectra. Standard, wide-field microscopy/spectroscopy is not a particularly effective tool for optically characterising tips. Instead, confocal hyperspectral imaging provides a viable method for mapping the local scattering response while broadband tuneable SERS offer a unique way of optically characterising the near-field. Incorporating these techniques into existing

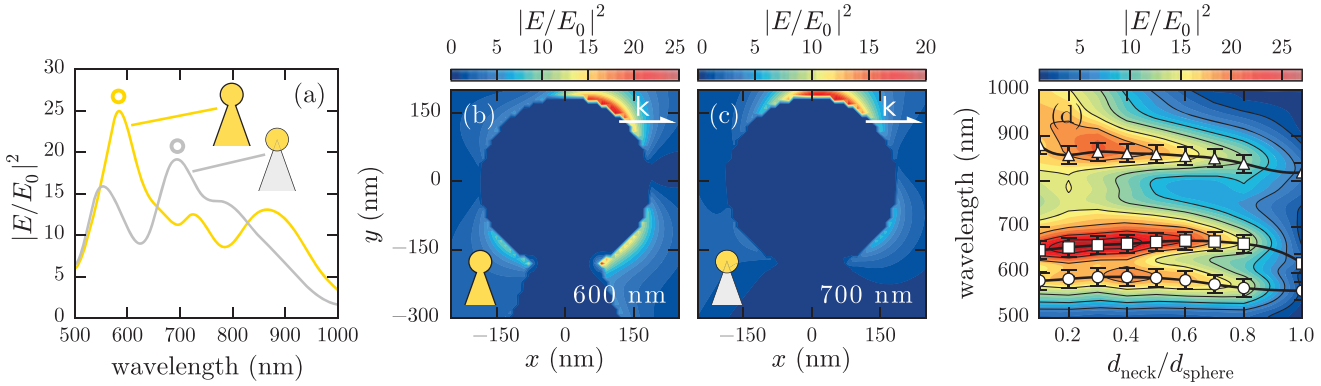

FIG. 4. (a) Numerically simulated near-field apex spectra of spherical Au and AuNP-on-Pt tips with (b), (c) near-field maps of the main resonance in each, as highlighted by circles in (a). Simulated tips have a 300 nm spherical radii, 120 nm neck widths, 20° opening angles, and 1.88 μm lengths to best match the typical experimental tip geometries and avoid truncation artefacts. Tips are illuminated by plane waves orientated along the tip axis. (d) Interpolated field enhancement map with superimposed resonant wavelengths, as the neck width varies from a spherical to a sharp tip. Tips have a 250 nm apex diameter, 1.88 μm length, and 10° opening angle.

microscopes is relatively simple and will greatly improve the reliability of tip-based near-field microscopy.

The authors thank EPSRC Grant Nos. EP/G060649/1, EP/K028510/1, and EP/L027151/1, and ERC Grant No. LINASS 320503 for funding and NanoTools for their services providing Au-coated spherical AFM tips. R.W.B. thanks Queens' College and the Royal Commission for the Exhibition of 1851 for financial support. Data generated as part of this work is available from the University of Cambridge repository http://dx.doi.org/10.17863/CAM.4682.

[1]R. Zhang, Y. Zhang, Z. Dong, S. Jiang, C. Zhang, L. Chen, L. Zhang, Y. Liao, J. Aizpurua, Y. Luo *et al.*, Nature **498**, 82 (2013).
[2]B. Pettinger, P. Schambach, C. J. Villagómez, and N. Scott, Annu. Rev. Phys. Chem. **63**, 379 (2012).
[3]W. Zhang, X. Cui, and O. J. Martin, J. Raman Spectrosc. **40**, 1338 (2009).
[4]M. I. Stockman, Phys. Rev. Lett. **93**, 137404 (2004).
[5]D. Pile and D. K. Gramotnev, Appl. Phys. Lett. **89**, 041111 (2006).
[6]S. Berweger, J. M. Atkin, R. L. Olmon, and M. B. Raschke, J. Phys. Chem. Lett. **1**, 3427 (2010).
[7]J. S. Lee, S. Han, J. Shirdel, S. Koo, D. Sadiq, C. Lienau, and N. Park, Opt. Express **19**, 12342 (2011).
[8]S. Berweger, J. M. Atkin, R. L. Olmon, and M. B. Raschke, J. Phys. Chem. Lett. **3**, 945 (2012).
[9]N. C. Lindquist, J. Jose, S. Cherukulappurath, X. Chen, T. W. Johnson, and S.-H. Oh, Laser Photonics Rev. **7**, 453 (2013).
[10]H. F. Hamann, A. Gallagher, and D. J. Nesbitt, Appl. Phys. Lett. **73**, 1469 (1998).
[11]C. Neacsu, G. Steudle, and M. Raschke, Appl. Phys. B **80**, 295 (2005).
[12]D. Mehtani, N. Lee, R. Hartschuh, A. Kisliuk, M. Foster, A. Sokolov, F. Čajko, and I. Tsukerman, J. Opt. A: Pure Appl. Opt. **8**, S183 (2006).
[13]C. A. Barrios, A. V. Malkovskiy, A. M. Kisliuk, A. P. Sokolov, and M. D. Foster, J. Phys. Chem. C **113**, 8158 (2009).
[14]B. Pettinger, K. F. Domke, D. Zhang, R. Schuster, and G. Ertl, Phys. Rev. B **76**, 113409 (2007).
[15]B. Pettinger, K. F. Domke, D. Zhang, G. Picardi, and R. Schuster, Surf. Sci. **603**, 1335 (2009).
[16]T. Mino, Y. Saito, and P. Verma, ACS Nano **8**, 10187 (2014).
[17]N. Hayazawa, Y. Inouye, Z. Sekkat, and S. Kawata, Chem. Phys. Lett. **335**, 369 (2001).
[18]E. Bailo and V. Deckert, Chem. Soc. Rev. **37**, 921 (2008).
[19]N. Hayazawa, T.-a. Yano, and S. Kawata, J. Raman Spectrosc. **43**, 1177 (2012).
[20]T. Umakoshi, T.-a. Yano, Y. Saito, and P. Verma, Appl. Phys. Express **5**, 052001 (2012).
[21]S. Kharintsev, G. Hoffmann, A. Fishman, and M. K. Salakhov, J. Phys. D: Appl. Phys. **46**, 145501 (2013).
[22]P. Uebel, S. T. Bauerschmidt, M. A. Schmidt, and P. S. J. Russell, Appl. Phys. Lett. **103**, 021101 (2013).
[23]A. Weber-Bargioni, A. Schwartzberg, M. Schmidt, B. Harteneck, D. Ogletree, P. Schuck, and S. Cabrini, Nanotechnology **21**, 065306 (2010).
[24]M. Fleischer, A. Weber-Bargioni, M. V. P. Altoe, A. M. Schwartzberg, P. J. Schuck, S. Cabrini, and D. P. Kern, ACS Nano **5**, 2570 (2011).
[25]I. Maouli, A. Taguchi, Y. Saito, S. Kawata, and P. Verma, Appl. Phys. Express **8**, 032401 (2015).
[26]Y. Zou, P. Steinvurzel, T. Yang, and K. B. Crozier, Appl. Phys. Lett. **94**, 171107 (2009).
[27]A. I. Denisyuk, M. A. Tinskaya, M. I. Petrov, A. V. Shelaev, and P. S. Dorozhkin, J. Nanosci. Nanotechnol. **12**, 8651 (2012).
[28]F. Huth, A. Chuvilin, M. Schnell, I. Amenabar, R. Krutokhvostov, S. Lopatin, and R. Hillenbrand, Nano Lett. **13**, 1065 (2013).
[29]A. Sanders, L. Zhang, R. W. Bowman, L. O. Herrmann, and J. J. Baumberg, Part. Part. Syst. Charact. **32**, 182 (2015).
[30]L. Herrmann, V. Valev, J. Aizpurua, and J. J. Baumberg, Opt. Express **21**, 32377 (2013).
[31]M. Bashevoy, F. Jonsson, Y. Chen, and N. Zheludev, Opt. Express **15**, 11313 (2007).
[32]M. I. Stockman, Opt. Express **19**, 22029 (2011).
[33]C. Huber, A. Trügler, U. Hohenester, Y. Prior, and W. Kautek, Phys. Chem. Chem. Phys. **16**, 2289 (2014).
[34]A. Lombardi, A. Demetriadou, L. Weller, P. Andrae, F. Benz, R. Chikkaraddy, J. Aizpurua, and J. J. Baumberg, ACS Photonics **3**, 471 (2016).
[35]J. T. Hugall and J. J. Baumberg, Nano Lett. **15**, 2600 (2015).
[36]K. J. Savage, M. M. Hawkeye, R. Esteban, A. G. Borisov, J. Aizpurua, and J. J. Baumberg, Nature **491**, 574 (2012).
[37]J. Mertens, A. L. Eiden, D. O. Sigle, F. Huang, A. Lombardo, Z. Sun, R. S. Sundaram, A. Colli, C. Tserkezis, J. Aizpurua *et al.*, Nano Lett. **13**, 5033 (2013).
[38]R. W. Taylor, F. Benz, D. O. Sigle, R. W. Bowman, P. Bao, J. S. Roth, G. R. Heath, S. D. Evans, and J. J. Baumberg, Sci. Rep. **4**, 5940 (2014).